BASIC AND TRANSLATIONAL—ALIMENTARY TRACT

In Vitro Expansion of Human Gastric Epithelial Stem Cells and Their Responses to Bacterial Infection

Sina Bartfeld,[1] Tülay Bayram,[1] Marc van de Wetering,[1,3] Meritxell Huch,[1] Harry Begthel,[1] Pekka Kujala,[2] Robert Vries,[1,3] Peter J. Peters,[2] and Hans Clevers[1]

[1]Hubrecht Institute for Developmental Biology and Stem Cell Research and University Medical Centre Utrecht, Utrecht; [2]Division of Cell Biology II, Antoni van Leeuwenhoek Hospital/Netherlands Cancer Institute, Amsterdam; and [3]Hubrecht Organoid Technology (HUB), Uppsalalaan 8, 3053DC, Utrecht, The Netherlands

BACKGROUND & AIMS: We previously established long-term, 3-dimensional culture of organoids from mouse tissues (intestine, stomach, pancreas, and liver) and human intestine and pancreas. Here we describe conditions required for long-term 3-dimensional culture of human gastric stem cells. The technology can be applied to study the epithelial response to infection with *Helicobacter pylori*. **METHODS:** We generated organoids from surgical samples of human gastric corpus. Culture conditions were developed based on those for the mouse gastric and human intestinal systems. We used microinjection to infect the organoids with *H pylori*. Epithelial responses were measured using microarray and quantitative polymerase chain reaction analyses. **RESULTS:** Human gastric cells were expanded indefinitely in 3-dimensional cultures. We cultured cells from healthy gastric tissues, single-sorted stem cells, or tumor tissues. Organoids maintained many characteristics of their respective tissues based on their histology, expression of markers, and euploidy. Organoids from healthy tissue expressed markers of 4 lineages of the stomach and self-organized into gland and pit domains. They could be directed to specifically express either lineages of the gastric gland, or the gastric pit, by addition of nicotinamide and withdrawal of WNT. Although gastric pit lineages had only marginal reactions to bacterial infection, gastric gland lineages mounted a strong inflammatory response. **CONCLUSIONS:** We developed a system to culture human gastric organoids. This system can be used to study *H pylori* infection and other gastric pathologies.

Keywords: Stomach Cancer; Gastric Epithelium; Primary Cells; Tissue Engineering.

The stomach is divided into 3 regions: the forestomach (in mice) or cardia (in human beings), the corpus, and the pyloric antrum. The human stomach lumen is lined with a monolayer of epithelial cells that is organized in flask-like invaginations, each of which consists of several glands that feed into a single luminal pit. The epithelium constantly renews itself and the stem cells fueling this process reside in the gastric glands.[1–4] Similar to the mouse intestine,[5,6] symmetric divisions and neutral drift leads to monoclonality of antral gastric units.[7] Mouse studies have proposed several markers for gastric stem cells.[4,8–11] Two markers, Lgr5 and Troy, have allowed the identification of cells that have the capacity to self-renew and to generate the different lineages of the stomach in vivo.[4,11]

Research on human gastric stem cells currently is limited. The analysis of spontaneous mutations in the cytochrome c oxidase gene has shown that some, but not all, human gastric units are monoclonal, allowing the conclusion that at one point in life multipotent stem cells have resided in these units.[3] However, direct evidence for the presence of multipotent gastric stem cells into adulthood is lacking.

One of the major functions of the gastrointestinal epithelium is to shield the body from infections and to maintain a peaceful co-existence with the gut commensals. Studies on host–pathogen or host–commensal interactions rely on the use of established model systems such as infection of animals or cancer cell lines,[12] but for many pathogens and commensals, such model systems have not been established yet.

The gastric pathogen *Helicobacter pylori* is one of the most successful pathogens. It uses a range of biological strategies to ensure persistency, which enables it to colonize the stomach of about half of the world's population.[13] Chronic infection can cause gastric ulcers and gastric cancer.[13] Currently, in vivo experimental studies use rodent models to understand *H pylori* infection. Although mouse studies certainly are useful, the clinical outcome of infection in mice is usually a mild gastritis that does not progress to ulceration or cancer. Alternatively, the Mongolian gerbil can develop cancer after *H pylori* infection, but these animals are outbred and the study of host factors therefore would be limited.[12] Other studies use gastric cancer cell lines that typically harbor oncogenic mutations. Human primary cells would represent the gastric epithelium much more closely, but current techniques are limited to isolation of differentiated (mostly mucous) cells that are not able to self-renew and thus can be maintained for only a few days.[14–16] No expanding primary gastric culture system exists that enables research of primary human gastric cells.

http://dx.doi.org/10.1053/j.gastro.2014.09.042

Here, we present a gastric culture system that allows indefinite (>1 y) expansion of human gastric cells. The cultures differentiate into the gastric lineages and can be used as a tool to study stem cell biology as well as the response of the epithelium to infection.

Materials and Methods

Human Tissue Material

Human corpus tissue was obtained from 17 patients (12 men, 5 women; age range, 41–87 y) who underwent partial or total gastrectomy at the University Medical Centre Utrecht. Ten patients were diagnosed with gastric cancer and 7 patients were diagnosed with esophageal cancer. This study was approved by the ethical committee of the University Medical Centre Utrecht. Samples were obtained with informed consent.

Organoid Culture

A detailed protocol for gastric culture is provided in the Supplementary materials. Briefly, glands were extracted from 1 cm^2 of human tissue using EDTA in cold chelation buffer,[17] seeded in Matrigel (BD Biosciences, Franklin Lakes, NJ), and overlaid with medium containing advanced Dulbecco's modified Eagle medium (DMEM)/F12 supplemented with penicillin/streptomycin, 10 mmol/L HEPES, GlutaMAX, 1 × B27 (all from Invitrogen, Waltham, MA), and 1 mmol/L N-acetylcysteine (Sigma-Aldrich, St Louis, MO). Growth factors were added to the basal medium as indicated in Figure 1 and Supplementary figure 1. The final human stomach culture medium contained the following essential components: 50 ng/mL epidermal growth factor (EGF) (Invitrogen), 10% noggin-conditioned medium, 10% R-spondin1–conditioned medium, 50% Wnt-conditioned medium, 200 ng/mL fibroblast growth factor (FGF)10 (Peprotech, Hamburg, Germany), 1 nmol/L gastrin (Tocris, Bristol, UK), and 2 μmol/L transforming growth factor (TGF)βi (A-83-01; Tocris). The facultative component was 10 mmol/L nicotinamide (Sigma-Aldrich). After seeding, 10 μmol/L rho-associated coiled coil forming protein serine/threonine kinase (RHOK) (Y-27632; Sigma-Aldrich) was added. Additional tested components were as follows: 100 ng/mL insulin-like growth factor (IGF) (Peprotech), 10 μmol/L p38 inhibitor (SB202190; Sigma-Aldrich), 3 μmol/L glykogensynthase-Kinase (GSK)3β inhibitor (CHIR99021; Axon Medchem, Groningen, The Netherlands), and 500 nmol/L prostaglandin E (PGE)2 (Tocris).

Approximately 1 cm^2 of cancer tissue was cut into small fragments and washed in cold chelation buffer until the supernatant was clear. Fragments were subjected to enzymatic digestion by 1.5 mg/mL collagenase (Gibco, Waltham, MA) and 20 μg/mL hyaluronidase (Sigma) in 10 mL advanced DMEM/F12 (Gibco), supplemented with antibiotics (Primocin; Invivogen, Toulouse, France), for 1 hour at 37°C with shaking. Cells were washed twice in advanced DMEM/F12, seeded into Matrigel, and overlayed with medium containing HEPES, GlutaMAX, penicillin, streptomycin, B27, n-acetylcysteine, EGF, R-spondin1, noggin, Wnt, FGF10, gastrin, TGFβ inhibitor, and RHOK inhibitor as described earlier.

Bacterial Culture and Infection

Bacterial culture conditions have been described previously.[18] Strains are specified in the Supplementary materials.

For infection studies, organoids were seeded in 50 μL Matrigel in 4-well multidishes (Thermo Scientific, Waltham, MA). Antibiotic-free medium was refreshed every 2–3 days, with a minimum of 3 medium changes before infection to allow removal of antibiotics from the culture. Organoids were microinjected on day 10 after seeding with an approximate multiplicity of infection (MOI) of 50 unless otherwise stated. For calculation of MOI, organoids were disrupted into single cells by EDTA and cells were counted (approximately 4000 cells/organoid). To achieve a final MOI of 50, bacteria were suspended in advanced DMEM/F12 at a density of $1 × 10^9$/mL and organoids were injected with approximately 0.2 μL bacterial suspension using a micromanipulator and microinjector (M-152 and IM-5B; Narishige, Tokyo, Japan) under a stereomicroscope (MZ75; Leica, Wetzlar, Germany) inside a sterile bench (CleanAir, Woerden, The Netherlands). For the viability test, organoids with injected bacteria were picked and each organoid was lysed in 200 μL Brain Heart Infusion (BHI) medium containing 0.5% saponin for 15 minutes with repeated pipetting. A total of 10 μL of 1:10 dilution rows were plated on horse serum agar plates. For heat inactivation, bacteria were kept at 56°C for 1 hour. To test inflammatory stimuli, organoids were incubated with medium containing the following substances in the final concentration: lipopolysaccharide (LPS) from *Escherichia coli* (1 μg/mL; Invivogen), recombinant human tumor necrosis factor (TNF)α (10 ng/mL; BD Pharmingen, Carlsbad, CA), recombinant human interleukin (IL)1β (100 ng/mL; Sigma-Aldrich), CpG oligodeoxynucleotide (ODN) 1668 (1 μg/mL; Enzo, Farmingdale, NY), and flagellin from *Salmonella typhimurium* (100 ng/mL; Invivogen).

The reader is referred to the Supplementary Materials and Methods section for fluorescence-activated cell sorting, polymerase chain reaction (PCR) and microarray, cell viability assay, karyotyping, histology, and imaging.

Results

Establishment of Human Stomach Cultures

To generate a culture system for human gastric epithelium, we isolated gastric glands from human gastric corpus tissue (Figure 1A) and observed their growth under different culture conditions. We started from the conditions for mouse gastric epithelium,[4] containing EGF, noggin, R-spondin1, Wnt, FGF10, and gastrin (ENRWFG). Isolated glands from human donors could form organoids in these conditions with very low efficiency and with a limited lifespan in vitro.

We then tested a panel of growth factors and inhibitors for organoid-forming efficiency, phenotype of the organoids, and longevity of the human gastric cultures. TGFβ inhibitor, p38 inhibitor, GSK2β inhibitor, and PGE2 were chosen because of the relevance of these respective pathways in cancer. IGF is expressed in normal gastric tissue.[10] Nicotinamide suppresses sirtuin activity.[19] Similar to human intestine,[17] nicotinamide increased the number of human gastric organoids formed (Figure 1B and Supplementary Figure 1A). It therefore was included in the subsequent culture condition (ENRWFGNi). IGF, p38 inhibitor, GSK3β inhibitor, and TGFβ inhibitor all induced budding structures in a concentration-dependent manner (Supplementary
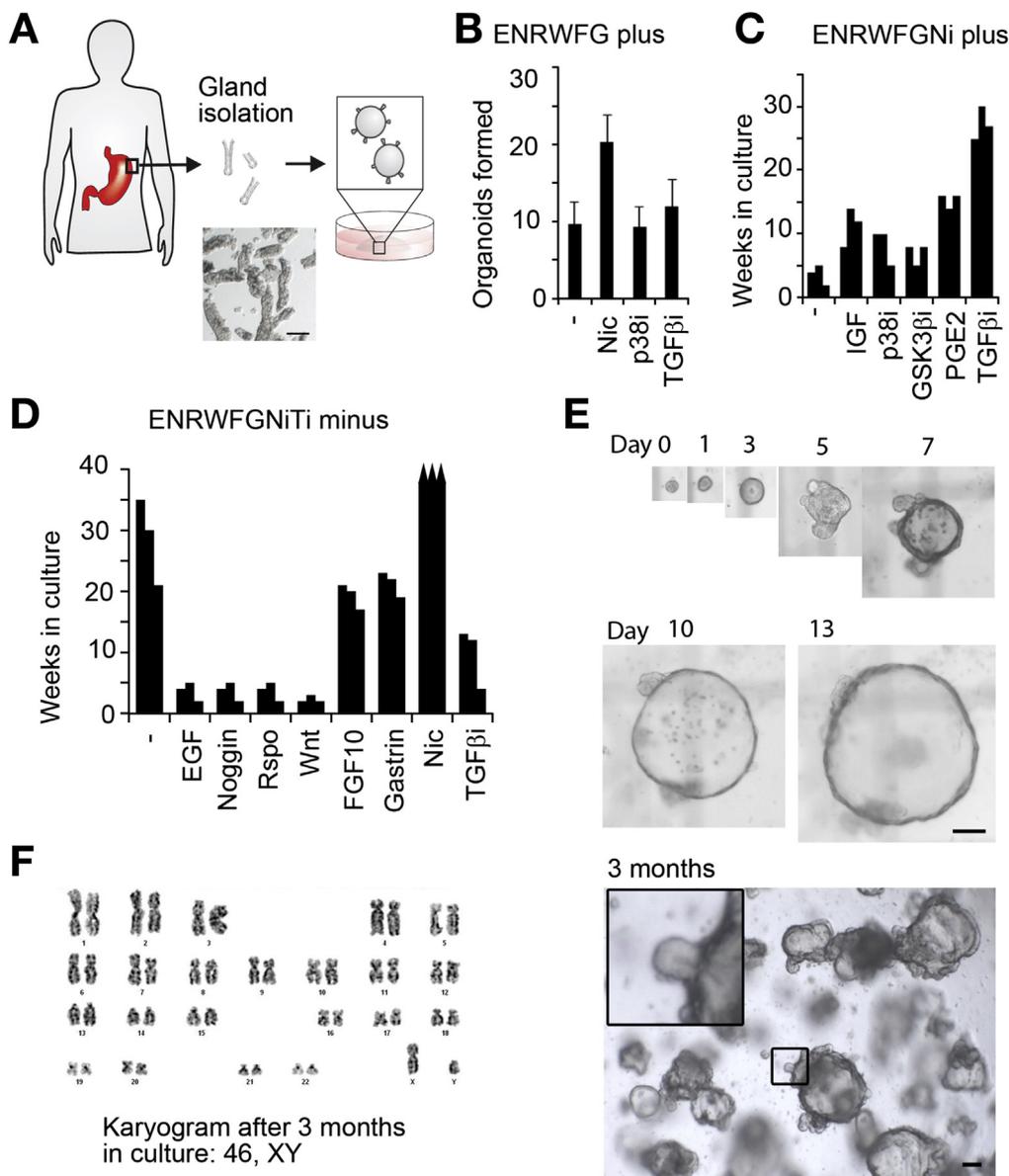
Figure 1. Human gastric cultures expand in vitro. (*A*) Scheme and image of gland isolation. (*B*) Nicotinamide (Nic) increases the formation of organoids, whereas the p38 inhibitor and the TGFβ inhibitor do not. *Bars* represent average of triplicates of one culture with standard deviation. (*C*) Effect of several growth factors and inhibitors on the human gastric culture. TGFβi increases the lifespan of organoids up to 30 weeks. (*D*) Removal of any of the factors EGF, noggin, R-spondin1, Wnt, FGF10, gastrin, or TGFβi limits the culture growth. Removal of nicotinamide enables long-term growth (>1 y). (*B* and *D*) Each bar represents a newly established culture. (*E*) Example of an organoid growing from a human gland. *Inset*: a budding structure. (*F*) Karyogram after 3 months in culture. *Scale bars*: 100 μm.

Figure 1*B*) and had a positive effect on the lifespan of the organoids (Figure 1*C*). PGE2 induced growth of large cysts and also prolonged the lifespan of the cultures. Addition of TGFβ inhibitor increased the lifespan to a maximum of half a year (Figure 1*C*), whereas all other factors had no such effect. We therefore only added TGFβ inhibitor (Ti) to the ENRWFGNi culture medium (ENRWFGNiTi). To analyze the importance of the single factors, we then withdrew each of the components from the medium. Without EGF, noggin, R-spondin1, or Wnt, organoid formation was strongly reduced and cultures deteriorated within 1–3 weeks (Figure 1*D* and Supplementary Figure 1*C*). Removal of FGF10, gastrin, or TGFβ inhibitor allowed growth for 10–20 weeks. Removal of nicotinamide increased the lifespan of the cultures (Figure 1*D*). Thus, the addition of nicotinamide promoted initial organoid formation, but limited the lifespan of the

cultures. We therefore used it as a facultative culture component.

The cultures developed in a stereotypical manner. After seeding, glands sealed and formed small cysts that subsequently expanded. Many organoids initially stayed cystic. With expansion of the culture, organoids became more uniform and consisted of several buddings that surrounded a central lumen (Figure 1*E*). Cultures were grown for 1 year with biweekly splitting rates of 1:5 without losing any of the features described. After 3 months of culture, chromosomal metaphase spreads of 2 patients were obtained and either 15 or 6 karyograms were aligned. There was no indication of chromosomal aberrations (Figure 1*F*). Organoids described here all were generated from corpus tissue. However, organoids also can be generated from cardia or pyloric antrum and expand
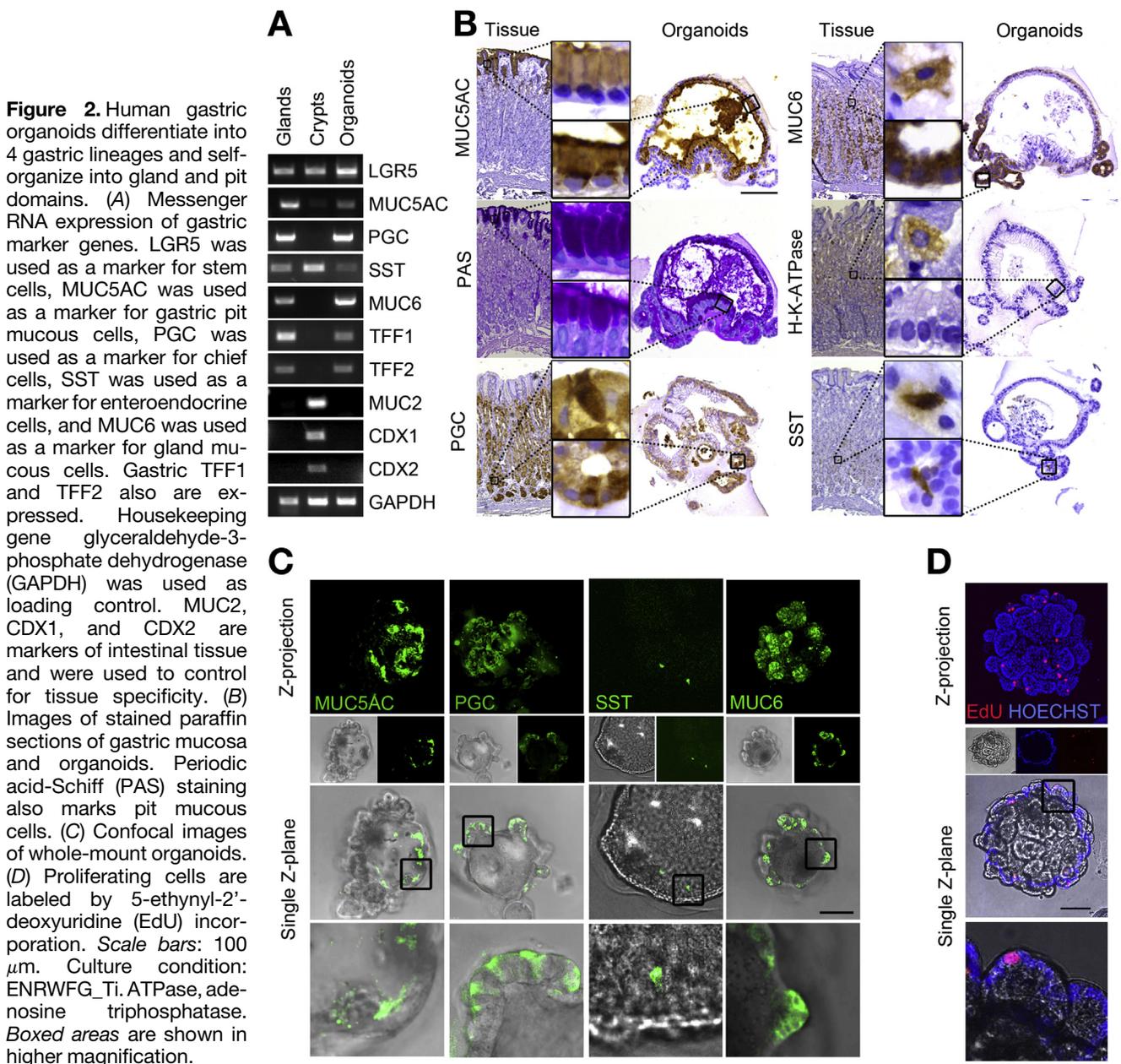
similarly under the culture conditions described here (tested for 3 months).

Human Gastric Organoids Differentiate Into Gastric Lineages and Self-Organize Into Gland and Pit Domains

We then analyzed the cellular composition of the organoids in the culture condition for optimal longevity (ENRWFG_Ti). PCR indicated that the organoids expressed the stem cell marker LGR5 as well as the gastric epithelial markers mucin 5AC (MUC5AC), pepsinogen (PGC), somatostatin (SST), mucin 6 (MUC6), trefoil factor 1 (TFF1), and trefoil factor 2 (TFF2). As expected for gastric cultures, they did not express the intestinal markers mucin 2 (MUC2), caudal-type homeobox (CDX) 1 and CDX2 (Figure 2A). As expected for organoids derived from the corpus region of the stomach, the antral markers gastrin and Pancreatic and duodenal homeobox (PDX)1 were not expressed according to microarray analysis comparing organoids with corpus and pyloric glands. Transcriptional profiling also indicated that markers of parietal cells and Enterochromaffin-like (ECL) cells, which usually are present in human corpus tissue, are not expressed in the organoids (microarray available online).

Histologic staining of paraffin sections as well as immunofluorescence staining of whole organoids showed remarkable organization. MUC5AC- and MUC6-positive mucous cells divided the organoids into gland and pit domains.

Figure 2. Human gastric organoids differentiate into 4 gastric lineages and self-organize into gland and pit domains. (A) Messenger RNA expression of gastric marker genes. LGR5 was used as a marker for stem cells, MUC5AC was used as a marker for gastric pit mucous cells, PGC was used as a marker for chief cells, SST was used as a marker for enteroendocrine cells, and MUC6 was used as a marker for gland mucous cells. Gastric TFF1 and TFF2 also are expressed. Housekeeping gene glyceraldehyde-3-phosphate dehydrogenase (GAPDH) was used as loading control. MUC2, CDX1, and CDX2 are markers of intestinal tissue and were used to control for tissue specificity. (B) Images of stained paraffin sections of gastric mucosa and organoids. Periodic acid-Schiff (PAS) staining also marks pit mucous cells. (C) Confocal images of whole-mount organoids. (D) Proliferating cells are labeled by 5-ethynyl-2'-deoxyuridine (EdU) incorporation. Scale bars: 100 μm. Culture condition: ENRWFG_Ti. ATPase, adenosine triphosphatase. Boxed areas are shown in higher magnification.

Although the budding structures consisted mostly of MUC6-positive mucous gland cells, the central lumen was lined with MUC5AC-positive mucous pit cells. PGC-positive chief cells and rare SST-positive enteroendocrine cells were scattered throughout the organoid (Figure 2B and C). Staining for H–K–adenosine triphosphatase was negative, confirming the absence of parietal cells (Figure 2B). Staining (5-ethynyl-2'-deoxyuridine) showed the presence of proliferative cells dispersed through the organoid (Figure 2D).

Directed Differentiation of Human Gastric Organoids to Gland or Pit Lineages

In the gastric mucosa, stem cells reside in the glands and produce progenitors that differentiate into pit cells as they migrate upward to the pit.[4] In the mouse stomach, expression of Wnt target genes (such as Troy, Lgr5, and Axin2) occurs in a gradient with high expression in the gland bottom and no expression in the pit.[11] We therefore hypothesized that it should be possible to generate organoids that only resemble the gland domains, whereas the progenitors can be directed toward the pit lineage by manipulating Wnt signal strength.

Comparing cultures with and without nicotinamide, staining of paraffin sections showed that the major effect of nicotinamide was the prevention of differentiation into MUC5AC-positive pit cells (Supplementary Figure 2). Thus, the condition ENRWFGNiTi generated organoids that lack the pit domain and only resemble the gland domains.

To direct these gland-type organoids to the pit lineage, we used a 2-step protocol: organoids were grown for 10 days in the full medium (ENRWFGNiTi) and then Wnt was withdrawn from the medium for 4 days to allow differentiation. During the differentiation phase, organoids underwent a phenotypical change, in becoming more cystic with less pronounced glands (Figure 3A). To globally assess the effect of Wnt withdrawal, we performed microarray analysis. As expected, Wnt was necessary for the expression of known stem cell markers such as LGR5 and TROY (Figure 3B). Moreover, removal of Wnt led to a decrease in expression of the chief cell marker PGC and the mucous neck cell marker MUC6. In turn, expression of the mucous pit cell marker MUC5AC was up-regulated (Figure 3B). The regulation of known Wnt pathway targets (LGR5, TROY, AXIN2, CD44[11]) as well as the expression of PGC, MUC6, and MUC5AC was confirmed by quantitative PCR (Figure 3C) and conventional PCR (Figure 3D). Gastric TFF1 and TFF2 also were expressed (Figure 3D). Markers of intestinal tissue (MUC2, CDX1, CDX2) were not expressed in organoids irrespective of the treatment (Figure 3D).

Staining of paraffin sections showed 2 distinct types of organoids. With Wnt, organoids resembled glands with MUC6-positive mucous gland cells in the buds and high numbers of PGC-positive chief cells but virtually no MUC5AC-positive pit cells (Figure 3E, left panel). Without Wnt, organoids had high numbers of MUC5AC pit cells, fewer PGC-positive chief cells, and only occasional MUC6-positive gland structures (Figure 3E, right panel). SST-positive enteroendocrine cells were very rare in all conditions. Quantification of the 4 cell lines in the 3 conditions confirmed the changes in cellular

composition of the organoids (Supplementary Figure 3). Thus, human gastric organoids can be directed into gland- or pit-type organoids, suggesting a potential role for a Wnt gradient in human gastric homeostasis (Figure 3F).

In summary, we can generate 3 different types of organoids that mostly differ in the composition of mucous-producing cells: (1) ever-expanding cultures of organoids that comprise 4 gastric lineages organized into gland and pit domains (complete type), in ENRWFG_Ti medium; (2) organoids with only gland domains (gland-type) in ENRWFGNiTi medium; and (3) organoids that consist of high numbers of pit cells (pit type) in ENR_FGNiTi medium.

Single Gastric Stem Cells Can Generate Organoids That Differentiate Into Four Lineages of the Stomach

To analyze the differentiation capacity of putative human gastric stem cells, we sorted single cells from gastric mucosa. For this, we plotted the cells using forward scatter area vs forward scatter peak linear and gated on the single-cell population (Figure 4A). The quality of the sort was confirmed by microscopic analysis. To increase organoid-forming efficiency and to avoid anoikis, we used nicotinamide and Rho kinase inhibitor for this experiment. 0.1% of the sorted cells formed organoids (Figure 4B) that could be expanded at a 1:5 ratio on a biweekly basis (Figure 4C). They expressed the gastric markers MUC5AC, PGC, SST, MUC6, TFF1, and TFF2, but not intestinal markers (MUC2, CDX1, and CDX2) as shown by PCR (Figure 4D). The cellular composition of single-cell–derived organoids was very similar to the one of gland-derived organoids as shown by immunohistochemistry. In the presence of Wnt and nicotinamide, organoids contain PGC-positive chief cells, MUC6-positive mucous neck cells, and very rare SST-positive enteroendocrine cells (gland-type organoids). After 4 days of Wnt withdrawal, MUC5AC-positive mucous pit cells appear (pit-type organoids) (Figure 4E). Quantifications corroborated these results (Supplementary Figure 3). In summary, we did not observe any differences between single-cell– and gland-derived organoids in terms of longevity, expansion rate, marker gene expression, or composition of cell types. Cultures shown in Figure 4E are 7 months old, showing that the different cell lineages are maintained over time. We conclude that the single cells behaved as multipotent stem cells.

In Vitro Expansion of Human Gastric Cancer Organoids

Treatment of gastric cancer patients depends on the availability of tests for drug discovery and sensitivity. Currently, gastric cancer cell lines are available, but no system allows comparison of cancerous and normal cells from the same patient. Having established the culture condition for human normal organoids, we reasoned that human gastric tumors also could be expanded under the same conditions. To establish the culture, cells were isolated from the tumor using collagenase and hyaluronidase, seeded into Matrigel, and embedded in ENRWFG_Ti medium. In parallel, organoids were established from normal
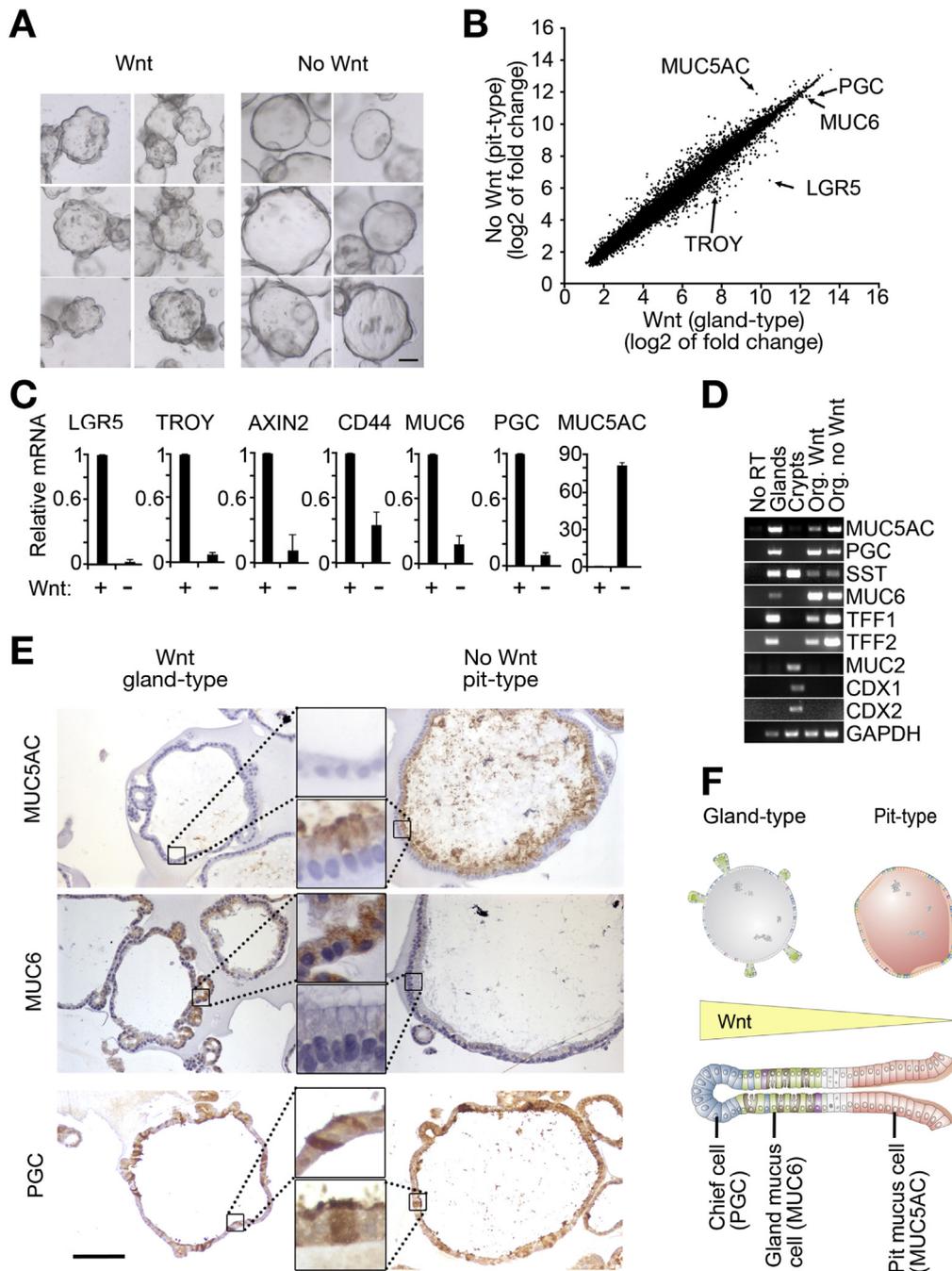
Figure 3. Directed differentiation of organoids into pit or gland cell lineages. (A) Examples of the phenotypical change at Wnt withdrawal. Cultures were grown in ENRWFGNiTi for 10 days and subsequently kept either with Wnt (*left panel*) or without Wnt (*right panel*) for 4 days. Cultures under Wnt withdrawal lose budding structures and become large cysts. (B) Differential gene expression in the 2 growth conditions measured by genome-wide microarray of cultures from 3 donors. Removal of Wnt reduces expression of stem cell markers (LGR5, TROY), and increases expression of MUC5AC. (C) Quantitative PCR of known Wnt response genes and stomach-specific genes. Messenger RNA (mRNA) was normalized to the GAPDH housekeeping gene. *Bars* represent the normalized average of triplicates with standard deviation. (D) PCR of gastric and intestinal markers. Intestinal markers MUC2, CDX1, and CDX2 are not expressed. (E) Images of stained paraffin sections show differential expression of MUC5AC and MUC6. PGC is expressed in both types of organoids. (F) Scheme of gastric gland and the 2 types of organoids. In all experiments, organoids were grown as described in panel A. *Scale bar*: 100 μm. GAPDH, glyceraldehyde-3-phosphate dehydrogenase.

tissue (Figure 5A). Chromosomal metaphase spreads were obtained from the tumor organoids (Figure 5B). Seven spreads were counted and showed aneuploidy with chromosome numbers between 70 and 160. Tumor cultures were reminiscent of the original tissue in terms of morphology shown by H&E staining and p53 accumulation as shown by p53 staining (Figure 5C, upper panel). To further analyze the possible mutation of the p53 pathway in

this tumor, we used nutlin-3, which inhibits the interaction between p53 and mouse double minute 2 homolog (MDM2) and thereby induces cell-cycle arrest. Nutlin-3 requires functional p53 and MDM2 for its activity, thus cancer cells with mutated p53 are not affected by this compound.[20] As expected, the normal organoids were strongly inhibited in their growth by nutlin-3, as quantified by a luciferase-based assay. In contrast, tumor organoids were insensitive to nutlin-3 treatment, indicating a mutated p53 pathway in this tumor (Figure 5D).

Infection of Human Gastric Cultures With H pylori Induces Inflammatory Response

In an infected individual, *H pylori* colonizes the lumen of the stomach and has contact with the apical side of the epithelium. In the organoids, the apical side of the polarized epithelium faces the lumen of the 3-dimensional structure. To enable bacteria to reach the natural side of infection, we established microinjection of the organoids (Figure 6A, *left*). Injection was confirmed by microscopy using GFP expressing *H pylori* and E-cadherin as an epithelial counterstain (Figure 6A, *right*). Plating of bacteria from organoids 2 hours after injection verified that the bacteria were alive inside the organoids (Supplementary Figure 4A and B). Electron microscopy showed that bacteria were engaged in very intimate contact with the epithelial cells (Figure 6B).

To determine the global primary response of the infected epithelium, we used microarray analysis. After 2 hours of infection, 25 genes were regulated 2-fold with a *P* value less than .05 (Supplementary Table 1). The highest up-regulated
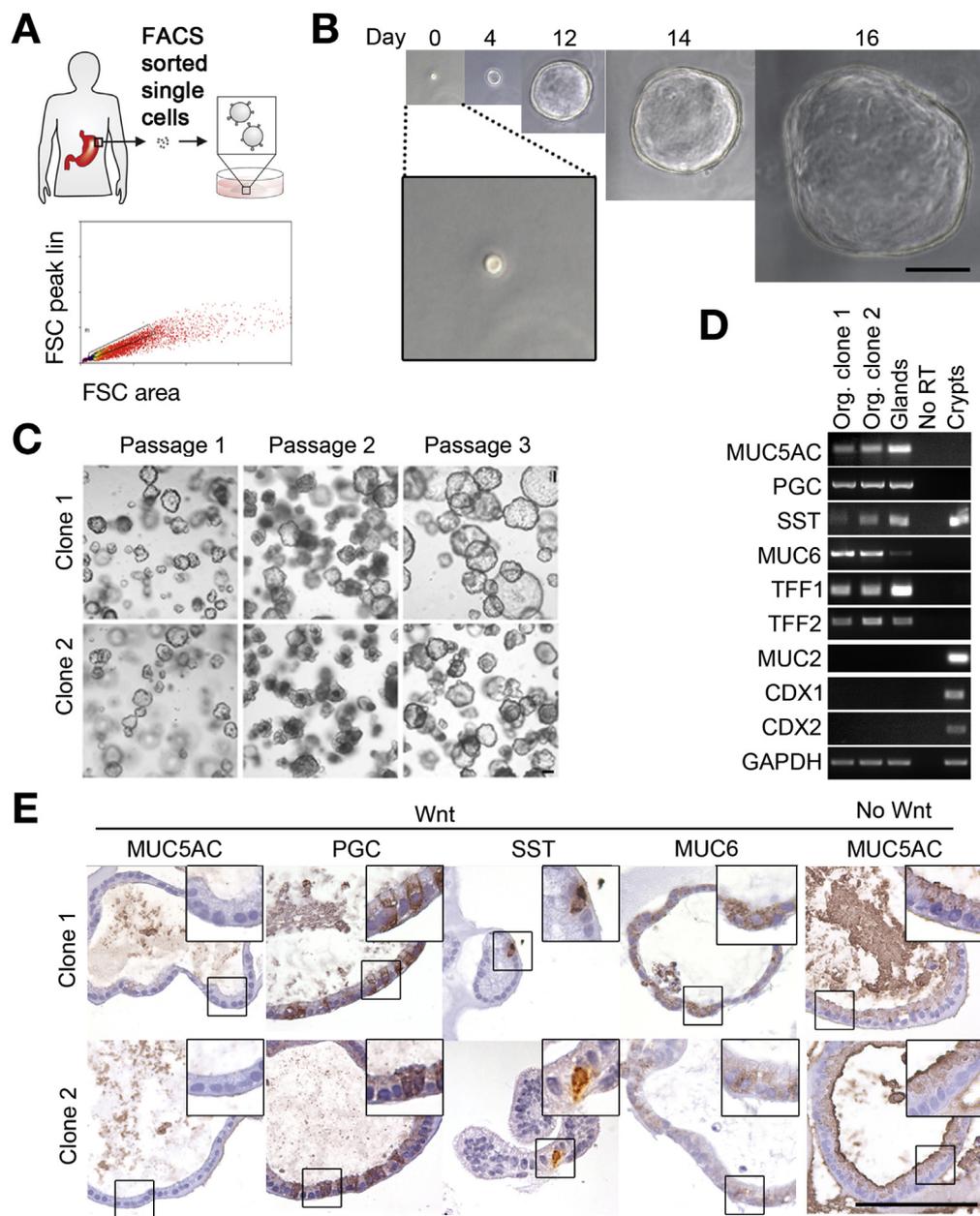

Figure 4. Single stem cells from human gastric mucosa can form gastric organoids. (A) Scheme of isolation and fluorescence-activated cell sorter (FACS) plot. FACS was used to generate single cells based on FSC. (B) Example of an organoid growing from a single cell. (C) Example of 2 single cell clones that were cultured for 1 year (the first 3 passages = 6 weeks). (D) Messenger RNA expression of gastric marker genes. Intestinal markers MUC2, CDX1, and CDX2 are not expressed and confirm tissue specificity. (E) Images of stained paraffin sections of organoids. MUC5AC expression increases after Wnt removal. Culture condition: ENRWFGNiTi (Wnt) or 4 days of Wnt withdrawal (no Wnt). *Scale bar*: 100 μm. *Boxed outlines* indicated areas that are shown in high magnification.
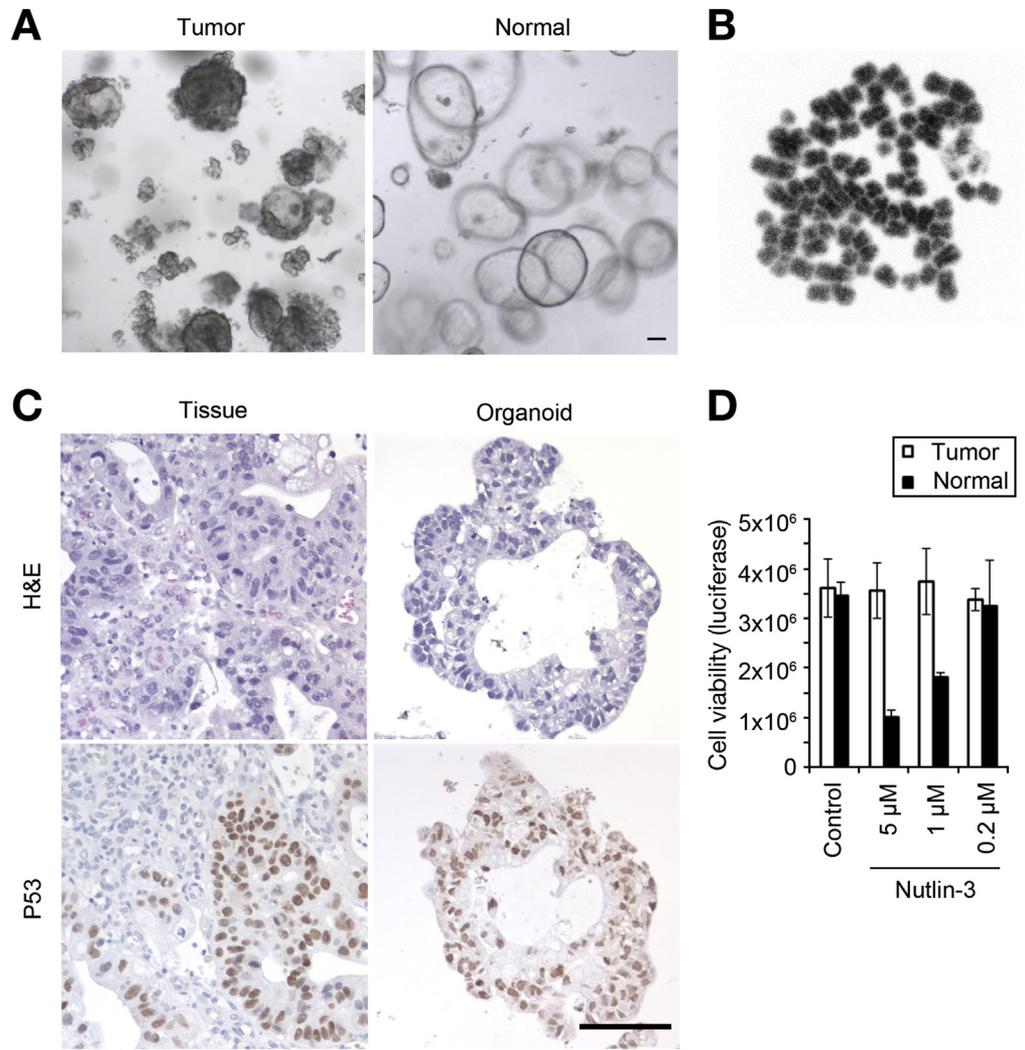
Figure 5. Normal and tumor organoids. (*A*) Brightfield image of tumor organoids (*left*) and normal organoids (*right*) established from the same patient. (*B*) Metaphase spread the tumor organoids shown in panel *A*. Counts of 7 spreads showed 70–160 chromosomes. (*C*) Images of stained paraffin sections of the original tumor tissue and organoids shown in panel *A*. (*D*) Organoids from the tumor are insensitive to nutlin-3. Organoids were grown for 1 week with the indicated concentrations of nutlin-3. Cell viability was assessed using luciferase assay. *Bars* represent the average of triplicates with standard deviation. *Scale bar*: 100 μm.

gene was human chorionic gonadotropin β chorionic gonadotropin β (CGB), a gene that has been associated with gastric cancer.[21] Many other highly up-regulated genes were targets of the nuclear factor-κB (NF-κB) pathway (Figure 6C), known to be activated in *H pylori* infection.[18,22,23] To test whether indeed this pathway was activated, we stained the NF-κB subunit p65 and found that after 1 hour of infection, p65 was translocated to the nuclei of the cells in infected organoids. Of note, neighboring organoids that did not contain bacteria did not show any p65 nuclear translocation (Figure 6D). A well-known target of NF-κB is the chemokine IL8, which attracts neutrophils and thereby promotes the inflammation.[24] Microarray analysis already indicated that IL8 was up-regulated in the organoids. Quantitative PCR of IL8 confirmed this. IL8 was not up-regulated in control organoids that were injected only with medium (mock) (Figure 6E). Induction of IL8 depended on the MOI (Supplementary Figure 4C). In human epithelial cell lines NF-κB activation depends on the cytotoxicity-associated gene pathogenicity island (*cag*PAI)

of the bacteria.[18,23] In human gastric organoids, IL8 expression did not depend on the *cag*PAI or on bacterial viability (Supplementary Figure 4D). Three *cag*PAI-independent stimuli have been reported to activate NF-κB via Toll-like receptors in *H pylori* infection: LPS, flagellin, or bacterial DNA.[23] Human gastric organoids are inert to purified LPS or CpG ODN (Supplementary Figure 4D), whereas these substances induce IL8 in other cells (data not shown). In contrast, organoids mount a strong IL8 response when incubated with purified flagellin or control TNFα and IL1β (Supplementary Figure 4D). Thus, generally, the organoids react to flagellin but are inert to LPS and CpG ODN. To analyze the importance of *H pylori* flagellum, we microinjected an aflagellated bacterial mutant. This mutant still induced IL8 expression, indicating that the bacterial flagellum is not the major inducer of IL8 in this system (Supplementary Figure 4E).

We then asked whether specific cells in the organoids respond to the bacteria and used our differentiation protocol to generate gland-type or pit-type organoids, which we
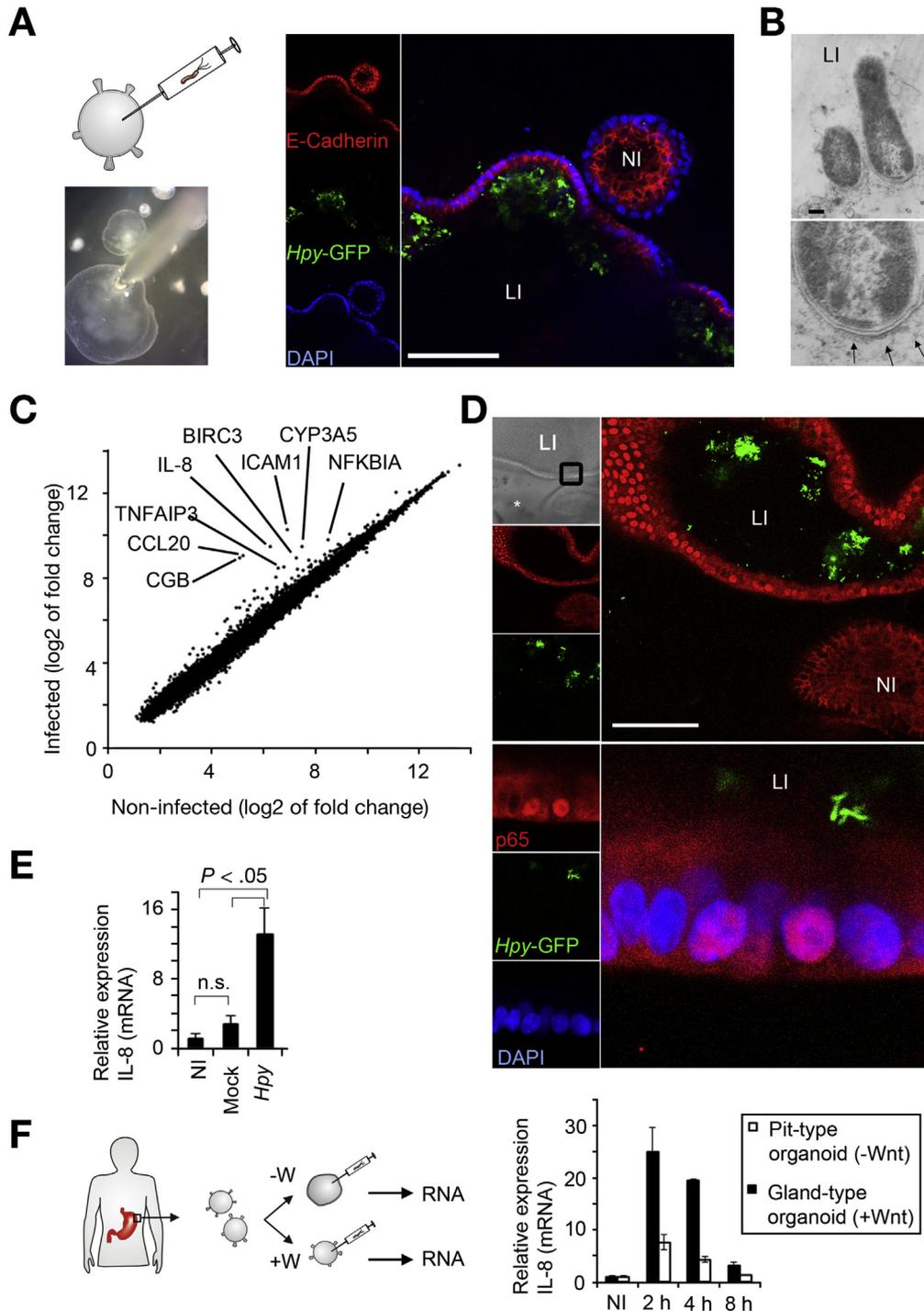
Figure 6. Primary response of gastric organoids to *H pylori* infection. (*A*) Scheme and brightfield image of microinjection of *H pylori* into an organoid (*left*). Confocal image of an infected organoid (lumen infected [LI]) and a noninfected organoid (NI) (*right*). Bacteria were visualized using GFP expression, organoids were counterstained with E-cadherin (red) and 4′,6-diamidino-2-phenylindol (DAPI) (blue). (*B*) Electron microscopy shows close interaction of bacteria with epithelial cells. *Arrows* indicate the binding site. (*C*) Differential gene expression upon infection of human gastric organoids. Genome-wide microarray was performed on 3 independent experiments using organoids derived from 3 patients. (*D*) Confocal images of infected (LI) and noninfected organoids (NI). Staining for NF-κB subunit p65 (red) indicates nuclear p65 in the infected organoid. (*E*) Quantitative PCR for IL8 messenger RNA (mRNA) after injection of *H pylori* or medium (mock). *Bars* represent the average of duplicates with standard deviation. (*F*) Organoids were differentiated into gland-type organoids (with Wnt) or pit-type organoids (4 days Wnt withdrawal) and subsequently microinjected with *H pylori*. After the indicated time, mRNA was extracted and the expression of IL8 was measured with quantitative real-time PCR. *Bars* represent the average of duplicates with standard deviation. *Scale bar*: (*B*) 200 nm or (*A* and *D*) 100 μm. *Matrigel.

subsequently microinjected with *H pylori*. IL8 expression was substantially higher in gland-type organoids than in pit-type organoids ([Figure 6](#)*F*).

Discussion

Here, we present a long-term 3-dimensional organoid culture system for primary, untransformed human gastric epithelium as well as human gastric cancer. By using this culture, we provide direct evidence for the presence of stem cells in adult human gastric tissue. The cells can be directed to differentiate into specific lineages of the stomach. The organoids mount an NF-κB–driven inflammatory response to infection and the strength of this response depends on the differentiated cell types in the organoids.

The presence of stem cells in the human adult stomach is expected, yet has not been shown previously. The organoids we present here can be grown from fluorescence-activated cell sorter–isolated single cells and generate 4 lineages of the stomach: pit mucous cells, gland mucous cells, chief cells, and enteroendocrine cells. Of the enteroendocrine cells, we identified SST-expressing cells, but not corpus-specific ECL cells. We also could not detect parietal cells. We assume the culture conditions were not optimal to allow differentiation into these cell types. Once clonal organoids are established, they expand without apparent limitation (>1 y), defying the Hayflick limit. Thus, the isolated cells can self-renew and are long-lived and multipotent, fulfilling the classic criteria for stem cells.

In the intestine, the pathologic activation of the Wnt pathway in cancer represents a deregulation of the controlled activation necessary for normal stem cell–driven tissue homeostasis.[25] In the stomach, the role of the Wnt pathway is less clear. Up to 30% of gastric tumors are found to carry an activated Wnt pathway,[26,27] whereas mutations in the Wnt pathway drive tumorigenesis in the mouse.[4,28] Two of the known stem cell markers in the mouse stomach, Troy and Lgr5, are Wnt target genes.[4,11] Here, we provide additional evidence for the importance of the Wnt pathway in human gastric epithelium. First, establishment and growth of human gastric organoids depends on Wnt and R-Spondin1. Second, on withdrawal of Wnt, organoids differentiate into pit lineage cultures. In the intestine, the Wnt-secreting Paneth cells provide the niche for stem cells[17] and competition for niche space determines the fate of the stem cell daughter cells.[5,6] It seems likely that there is a Wnt source at the bottom of gastric glands and that the migration of daughter cells upward toward the gastric surface directs the differentiation into the pit lineage.

We used human organoids to analyze the primary response of the human epithelium to *H pylori* and find robust NF-κB activation. *H pylori* has been shown to activate this transcription factor in various human and murine cell lines.[18,22,23,29] In addition, a study using short-lived human primary mucous cells showed induction of IL8.[30] Results here indicate that in human organoids, IL8 expression is independent of bacteria viability and independent of Toll-like receptor 4, 5, and 9 signaling. Further studies are needed to analyze the precise signaling pathways leading to NF-κB activation in this system. The human organoids allow

us to further compare the NF-κB response in cells of the pit and the gland lineages. We find that the gland lineages respond with higher amounts of IL8 than the pit lineage. This is in line with earlier studies that analyzed the importance of bacterial chemotaxis in infection. These studies found that wild-type bacteria can colonize the gastric glands, but bacterial mutants with defects in chemotaxis were only able to colonize the surface mucus. After months of infection, the bacteria in the glands had induced a higher inflammation and T-cell response than the bacteria in the surface layer.[31,32] Our finding also was in line with the general idea that the gastroepithelial lining protects itself from chronic inflammation by creating a certain "blindness" on the surface.[33] Two mechanisms are likely to underlie the relatively low response of the gastric surface cells observed here, as follows: (1) the surface cells promote physical separation from the bacteria by forming a thick mucus layer, and (2) the host restricts receptors initiating the NF-κB response to the deeper glands, which should be less in contact with bacteria.[33,34] Future research has to determine whether one or both (or a now not anticipated mechanism) restricts the pit cell inflammatory response.

In summary, the organoids described here present a new model of self-renewing gastric epithelium grown from stem cells that can be directed into the different lineages of the stomach. It represents a model that is much closer to the gastric epithelium than currently used cell lines. Organoids can be grown from surgical resections as well as from biopsy specimens and can be expanded without apparent growth limitation. This method also allows growth of parallel samples from normal as well as cancerous gastric cells from the same patient. This will enable their use for future patient-derived disease models, drug screens, gastric stem cell research, and for the study of host pathogen interactions.

Supplementary Material

References

1. Karam SM, Leblond CP. Dynamics of epithelial cells in the corpus of the mouse stomach. I. Identification of proliferative cell types and pinpointing of the stem cell. Anat Rec 1993;236:259–279.
2. Bjerknes M, Cheng H. Multipotential stem cells in adult mouse gastric epithelium. Am J Physiol Gastrointest Liver Physiol 2002;283:G767–G777.
3. McDonald SAC, Greaves LC, Gutierrez–Gonzalez L, et al. Mechanisms of field cancerization in the human stomach: the expansion and spread of mutated gastric stem cells. Gastroenterology 2008;134:500–510.
4. **Barker N, Huch M**, Kujala P, et al. Lgr5+ve stem cells drive self-renewal in the stomach and build long-lived gastric units in vitro. Cell Stem Cell 2010;6:25–36.
5. Snippert HJ, van der Flier LG, Sato T, et al. Intestinal crypt homeostasis results from neutral competition

between symmetrically dividing Lgr5 stem cells. Cell 2010;143:134–144.

6. Ritsma L, Ellenbroek SIJ, Zomer A, et al. Intestinal crypt homeostasis revealed at single-stem-cell level by in vivo live imaging. Nature 2014;507:362–365.

7. Leushacke M, Ng A, Galle J, et al. Lgr5+ gastric stem cells divide symmetrically to effect epithelial homeostasis in the pylorus. Cell Rep 2013;5:349–356.

8. Qiao XT, Ziel JW, McKimpson W, et al. Prospective identification of a multilineage progenitor in murine stomach epithelium. Gastroenterology 2007;133:1989–1998.e3.

9. Arnold K, Sarkar A, Yram MA, et al. Sox2+ adult stem and progenitor cells are important for tissue regeneration and survival of mice. Cell Stem Cell 2011;9:317–329.

10. Mills JC, Andersson N, Hong CV, et al. Molecular characterization of mouse gastric epithelial progenitor cells. Proc Natl Acad Sci U S A 2002;99:14819–14824.

11. Stange DE, Koo B-K, Huch M, et al. Differentiated Troy+ chief cells act as reserve stem cells to generate all lineages of the stomach epithelium. Cell 2013;155:357–368.

12. O'Rourke JL, Lee A. Animal models of Helicobacter pylori infection and disease. Microbes Infect 2003;5:741–748.

13. Salama NR, Hartung ML, Müller A. Life in the human stomach: persistence strategies of the bacterial pathogen Helicobacter pylori. Nat Rev Microbiol 2013;11:385–399.

14. Takahashi M, Ogura K, Maeda S, et al. Promoters of epithelialization induce expression of vascular endothelial growth factor in human gastric epithelial cells in primary culture. FEBS Lett 1997;418:115–118.

15. Richter-Dahlfors A, Heczko U, Meloche RM, et al. Helicobacter pylori-infected human antral primary cell cultures: effect on gastrin cell function. Am J Physiol 1998;275:G393–G401.

16. Krueger S, Hundertmark T, Kuester D, et al. Helicobacter pylori alters the distribution of ZO-1 and p120ctn in primary human gastric epithelial cells. Pathol Res Pract 2007;203:433–444.

17. Sato T, Stange DE, Ferrante M, et al. Long-term expansion of epithelial organoids from human colon, adenoma, adenocarcinoma, and Barrett's epithelium. Gastroenterology 2011;141:1762–1772.

18. Bartfeld S, Hess S, Bauer B, et al. High-throughput and single-cell imaging of NF-kappaB oscillations using monoclonal cell lines. BMC Cell Biol 2010;11:21.

19. Denu JM. Vitamin B3 and sirtuin function. Trends Biochem Sci 2005;30:479–483.

20. Tovar C, Rosinski J, Filipovic Z, et al. Small-molecule MDM2 antagonists reveal aberrant p53 signaling in cancer: implications for therapy. Proc Natl Acad Sci U S A 2006;103:1888–1893.

21. Yakeishi Y, Mori M, Enjoji M. Distribution of beta-human chorionic gonadotropin-positive cells in noncancerous gastric mucosa and in malignant gastric tumors. Cancer 1990;66:695–701.

22. Viala J, Chaput C, Boneca IG, et al. Nod1 responds to peptidoglycan delivered by the Helicobacter pylori cag pathogenicity island. Nat Immunol 2004;5:1166–1174.

23. Ferrero RL. Innate immune recognition of the extracellular mucosal pathogen, Helicobacter pylori. Mol Immunol 2005;42:879–885.

24. Shimoyama T, Crabtree J. Bacterial factors and immune pathogenesis in Helicobacter pylori infection. Gut 1998;43:S2–S5.

25. Clevers H. The intestinal crypt, a prototype stem cell compartment. Cell 2013;154:274–284.

26. Horii A, Nakatsuru S, Miyoshi Y, et al. The APC gene, responsible for familial adenomatous polyposis, is mutated in human gastric cancer. Cancer Res 1992;52:3231–3233.

27. Clements WM, Wang J, Sarnaik A, et al. β-Catenin mutation is a frequent cause of Wnt pathway activation in gastric cancer. Cancer Res 2002;62:3503–3506.

28. Radulescu S, Ridgway RA, Cordero J, et al. Acute WNT signalling activation perturbs differentiation within the adult stomach and rapidly leads to tumour formation. Oncogene 2013;32:2048–2057.

29. Bauer B, Moese S, Bartfeld S, et al. Analysis of cell type-specific responses mediated by the type IV secretion system of Helicobacter pylori. Infect Immun 2005;73:4643–4652.

30. Ogura K, Takahashi M, Maeda S, et al. Interleukin-8 production in primary cultures of human gastric epithelial cells induced by Helicobacter pylori. Dig Dis Sci 1998;43:2738–2743.

31. Howitt MR, Lee JY, Lertsethtakarn P, et al. ChePep controls Helicobacter pylori infection of the gastric glands and chemotaxis in the epsilonproteobacteria. MBio 2011;2:e00098-11.

32. Rolig AS, Carter JE, Ottemann KM. Bacterial chemotaxis modulates host cell apoptosis to establish a T-helper cell, type 17 (Th17)-dominant immune response in Helicobacter pylori infection. Proc Natl Acad Sci U S A 2011;108:19749–19754.

33. Pédron T, Sansonetti P. Commensals, bacterial pathogens and intestinal inflammation: an intriguing ménage à trois. Cell Host Microbe 2008;3:344–347.

34. Abreu MT, Fukata M, Arditi M. TLR signaling in the gut in health and disease. J Immunol 2005;174:4453–4460.

Supplementary Materials and Methods

Bacterial Strains and Culture

H pylori P12 and G27 are clinical isolates.[1,2] P12-GFP is a GFP-expressing derivate.[3] P12Δ*cag*PAI lacks the pathogenicity island.[3] G27Δ*fliG* is aflagellated.[4] G27Δ*motB* is nonmotile.[5] P12 and derivates were a kind gift from Thomas F. Meyer. G27 and derivates were a kind gift from Karen Ottemann. Bacteria were grown on agar plates (GC agar; BD) supplemented with 10% horse serum (Gibco), vancomycin (10 μg/mL), trimethoprim (5 μg/mL), and nystatin (1 μg/mL) under microaerobic conditions (85% N_2, 10% CO_2, 5% O_2) at 37°C. For the mutant bacteria, kanamycin (8 μg/mL) or chloramphenicol (4 μg/mL) was added as applicable.

PCR and Microarray

RNA was prepared from organoids, isolated gastric glands, or isolated intestinal crypts according to the manufacturer's recommendations (RNeasy Mini kit; Qiagen, Venlo, Netherlands). Complementary DNA was generated using reverse transcriptase (Promega). Quantitative real-time PCR was performed using SYBR green (Bio-Rad) and the CFX 384 Real Time system (Bio-Rad). Results were calculated by using the ΔΔCt method in Excel (Microsoft). Relative quantification was achieved by normalizing the values of the glyceraldehyde-3-phosphate dehydrogenase (GAPDH) gene. Nonquantitative PCRs were performed using the same primers. Microarray (Affymetrix) analysis was performed on a genome-wide messenger RNA expression platform (Human Gene ST 2.0; Affymetrix). Data were analyzed using the R2 web application (available: http://r2.amc.nl). The data were deposited in the GEO database: accession number GSE60557.

Primers used for PCR and quantitative PCR were as follows: MUC5AC: 5'-CTTCTCAACGTTTGACGGGAAGC-3' and 5'-CTTGATCACCACCACCGTCTG-3'; MUC6: 5'-GCCCCGGTAT CTTCTCTCGG-3' and 5'-ACACCTGCAGGGTGAGTACG-3'; PGC: 5'-AGAGCCAGGCCTGCACCAGT-3' and 5'-GCCCCTGTGGCC TGCAGAAG-3'; SST: 5'-CTAGAGTTTGACCAGCCAC-3' and 5'-GACAGATCTTCAGGTTCCAG-3'; LGR5: 5'-TATGCCTTTGGAA ACCTCTC-3' and 5'-CACCATTCAGAGTCAGTGTT-3'; TNFR SF19: 5'-CTGCTCATCCTCTGTGTCATCTATTG-3' and 5'-CCGTTGTACTGAATGTCCTGTG-3'; CD44: 5'-AGATGGAGAA AGCTCTGAGC-3' and 5'-GTAATTGGTCCATCAAAGGC-3'; AXI N2: 5'-ACTTCAAGTGCAAACTTTCG-3' and 5'-GGAAATGAGG TAGAGACAC-3'; IL8: 5'-ACACTGCGCCAACACAGAAAT-3' and 5'-ATTGCATCTGGCAACCCTACA-3'; GAPDH: 5'-GGTATCGTG GAAGGACTCATGAC-3' and 5'-ATGCCAGTGAGCTTCCCGTT CAG-3'; CDX1: 5'-GTGGCAGCGGTAAGACTC-3' and 5'-GTTCA CTTTGCGCTCCTTTGC-3'; CDX2: 5'-AACCAGGACGAAAGA CAAAT-3' and 5'-GAAGACACCGGACTCAAG-3'; TFF1: 5'-CCATGGAGAACAAGGTGAT-3' and 5'-CACCAGGAAAACCA CAATTC-3'; and TFF2: 5'-GACAATGGATGCTGTTTCG-3' and 5'-GTAATGGCAGTCTTCCACAGA-3'.

Fluorescence-Activated Cell Sorting

Single cells were sorted using MoFlo (Beckman Coulter). Isolated glands were prepared as described earlier, incubated in 10 mmol/L EDTA, and pipetted through a pointed glass pipette until most of the cells were single. Before fluorescence-activated cell sorting, cells were passed through a 20-μm cell strainer and washed with cold basal medium. Dead cells were excluded by propidium iodide staining. Single cells were gated by using forward scatter area vs forward scatter peak linear. This does not enrich for stem cells but was used to generate single cells.

Histology and Imaging

Organoids and tissue samples were fixed with 4% FA overnight at 4°C. Paraffin sections and immunohistochemistry were generated as previously described.[6] For whole-mount analysis, organoids were permeabilized with 0.3% Triton X-100 (Sigma) and stained in phosphate-buffered saline 0.3% Triton, 1% bovine serum albumin, and 5% normal goat serum (with the exception of the anti-PGC antibody in which bovine serum albumin was omitted because of cross-reactivity). The following antibodies were used: MUC5AC (45M1; Vision Biosystems, now Leica Microsystems, Wetzlar, Germany.), MUC6 (T20 sc16914; Santa Cruz, Dallas, TX), PGC (ab9013; Abcam, Cambridge, UK), SST (18-0078; Invitrogen), E-cadherin (610405; BD Transduction Labs, Carlsbad, CA.), p65 (sc109; Santa Cruz). DNA was stained with 4',6-diamidino-2-phenylindol (Molecular Probes, Waltham, MA). Staining (5-ethynyl-2'-deoxyuridine) was performed according to the manufacturer's recommendations (Click-It; Invitrogen). Images were taken using standard or confocal microscopy (Eclipse E600; Nikon, Chiyoda, Japan; or DMIL or SP5; Leica). Cell lineages were counted based on staining as performed previously.[7] Images were taken on a Nikon Eclipse E600, and cells were counted in a blinded fashion in 7 images, each containing at least 1 organoid and a total of 500 cells per condition and staining.

Karyotyping

Metaphase spreads were generated after 24 hours of colcemid treatment (0.1 μg/mL; Gibco). Organoids were removed from Matrigel and dissociated into single cells using trypsin. Cells were lysed with 0.075 mol/L KCL and material was fixed using methanol:acetic acid (3:1). For normal tissue, organoid lines from 2 patients (either 6 or 15 spreads) were karyotyped by the Laboratory for Cytogenetics in the Wilhelmina Children's Hospital in Utrecht using Case Data Manager software (Applied Spectral Imaging, Carlsbad, CA). For tumor tissue, 7 metaphase spreads as shown in Figure 5B were counted from 1 organoid line.

Cell Viability Assay

Cell viability was analyzed using a luminescent cell viability assay (CellTiter-Glo; Promega) according to the manufacturer's recommendations. The assay is based on quantitation of the adenosine triphosphate present, which is an indication of the viable cells. Briefly, each well of a 48-well plate of organoids was lysed in 200 μL reagents, mixed thoroughly, and incubated for 10 minutes. A total of 20 μL of the mix was transferred to a clean, white-bottom, 96-well plate and luminescence was measured. Data were compiled in Excel (Microsoft).
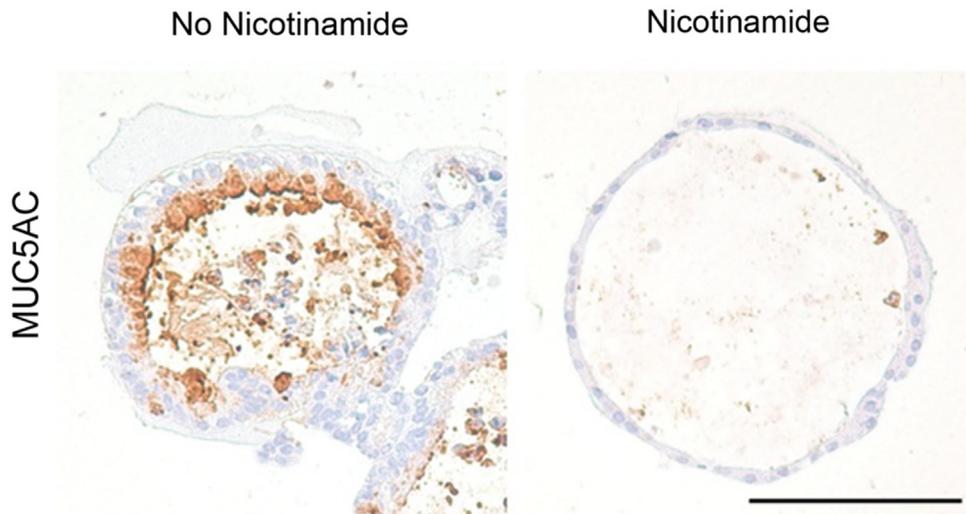
Supplementary References

1. Odenbreit S, Till M, Haas R. Optimized BlaM-transposon shuttle mutagenesis of Helicobacter pylori allows the identification of novel genetic loci involved in bacterial virulence. Mol Microbiol 1996;20:361–373.

2. Censini S, Lange C, Xiang Z, et al. cag, a pathogenicity island of Helicobacter pylori, encodes type I-specific and disease-associated virulence factors. Proc Natl Acad Sci U S A 1996;93:14648–14653.

3. Wunder C, Churin Y, Winau F, et al. Cholesterol glucosylation promotes immune evasion by Helicobacter pylori. Nat Med 2006;12:1030–1038.

4. Lowenthal AC, Hill M, Sycuro LK, et al. Functional analysis of the Helicobacter pylori flagellar switch proteins. J Bacteriol 2009;191:7147–7156.

5. Ottemann KM. Helicobacter pylori uses motility for initial colonization and to attain robust infection. Infect Immun 2002;70:1984–1990.

6. Batlle E, Henderson JT, Beghtel H, et al. β-Catenin and TCF mediate cell positioning in the intestinal epithelium by controlling the expression of EphB/ephrinB. Cell 2002;111:251–263.

7. Xiao C, Feng R, Engevik AC, et al. Sonic Hedgehog contributes to gastric mucosal restitution after injury. Lab Invest 2012;93:96–111.
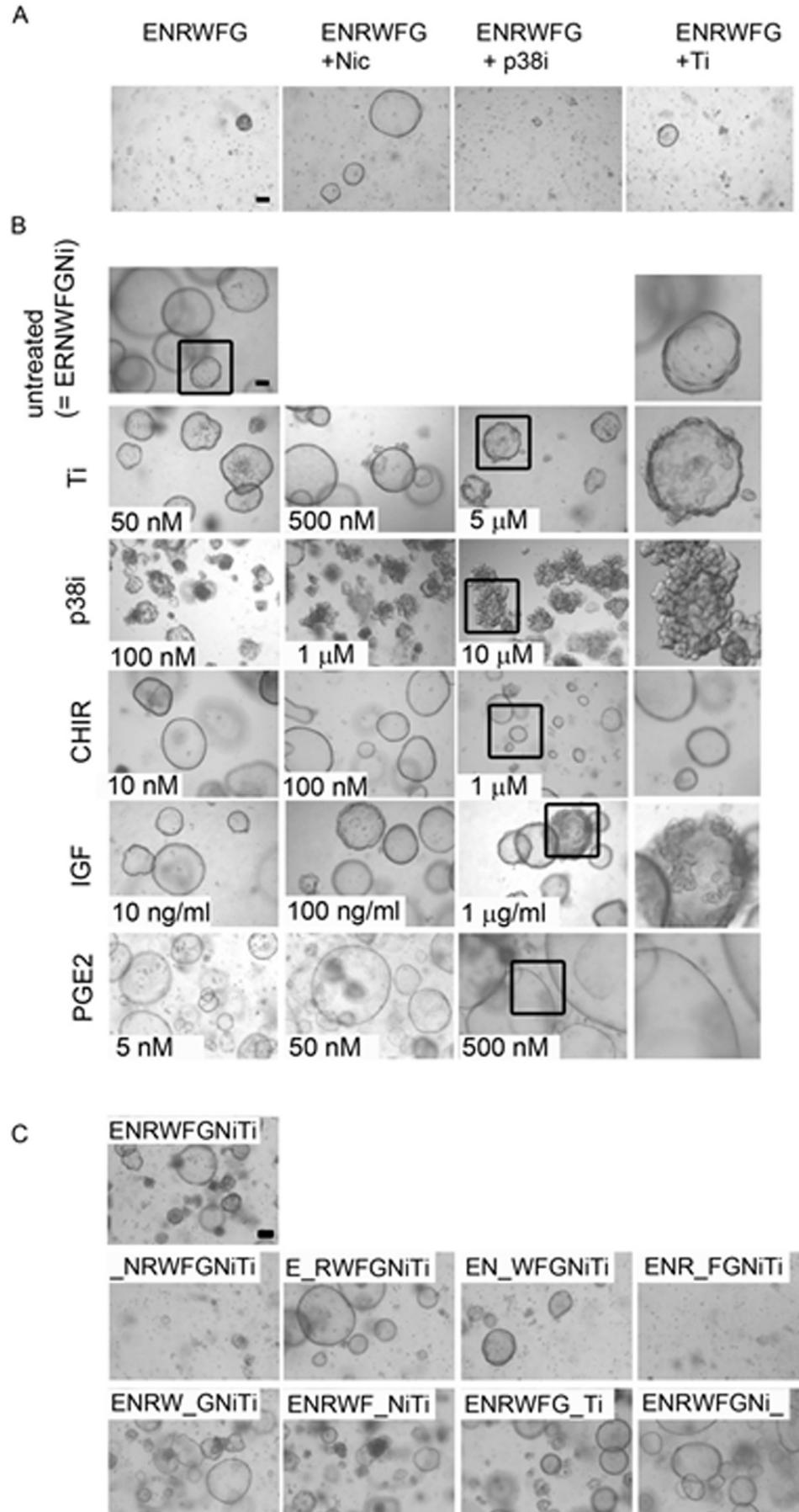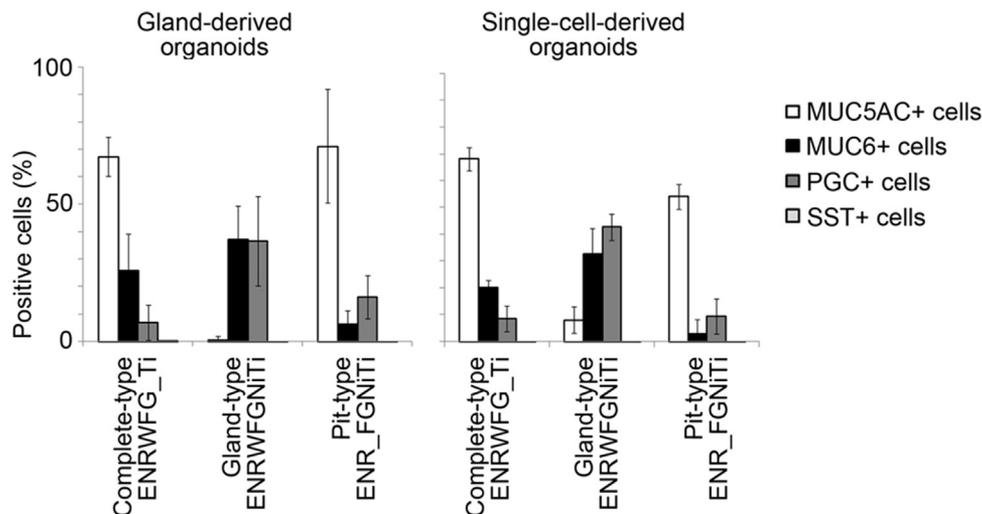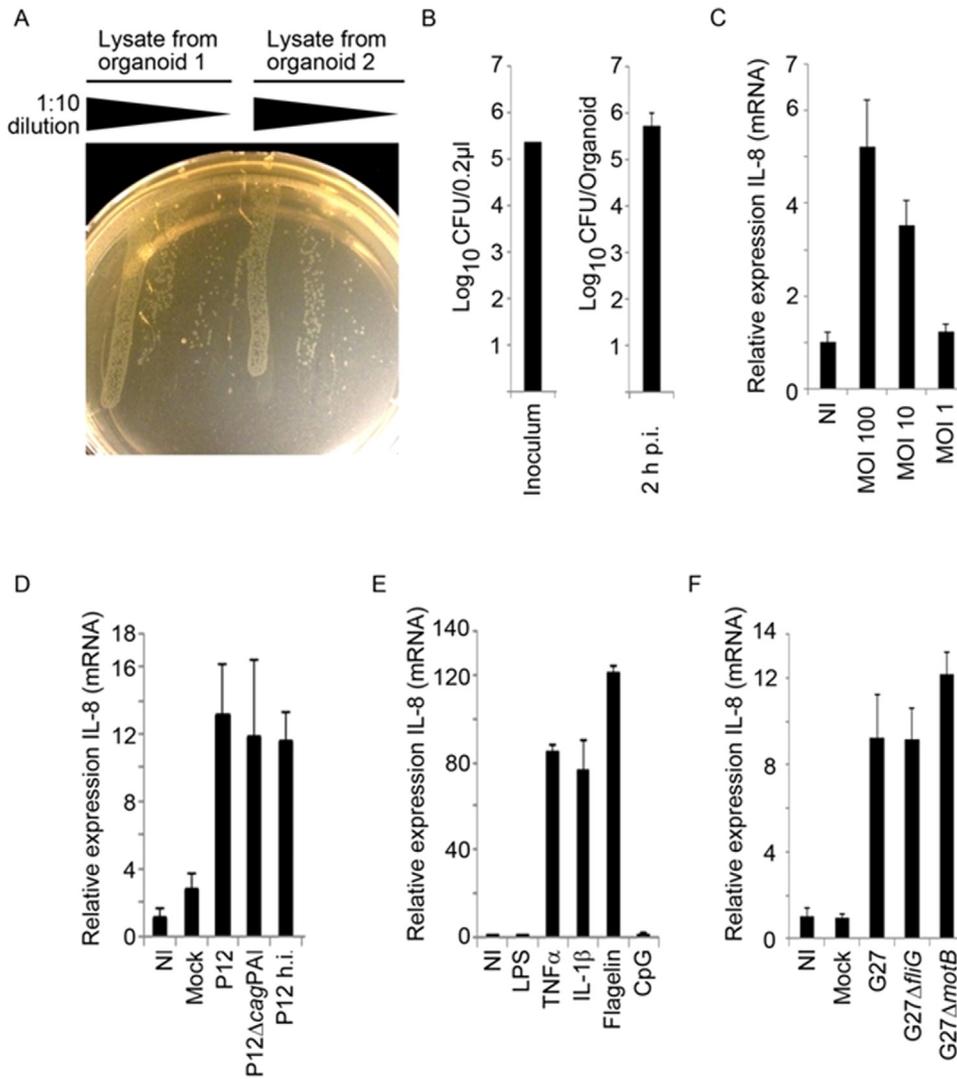
Supplementary
Figure 1. Establishing growth conditions for human gastric organoids. (*A*) Nicotinamide (Nic) supports organoid formation after 10 days. (*B*) Phenotypical changes and titration of growth factor concentration. High concentrations of TGFβ inhibitor (Ti), p38 inhibitor, or IGF increases budding structures. GSK3beta inhibitor (CHIR) decreases organoid size. PGE2 induces large cysts. (*C*) Formation of organoids in incomplete media. Wnt is essential for initial growth (ENR_FGNiTi). Cultures lacking other factors show already reduced organoid formation (compare Figure 1E). *Scale bars*: 100 μm. ENRWFGNiTi, EGF, R-spondin1, Noggin, Wnt, FGF10, gastrin, nicotinamide, and TGFβ-inhibitor. *Boxes* indicate the areas that are shown in higher magnification in the *right panel*.

No Nicotinamide

Nicotinamide

MUC5AC

Supplementary Figure 2. Nicotinamide suppresses differentiation into mucous pit cell lineage. Images of stained paraffin sections of organoids. Cells were grown in either ENRWFG_Ti or ENRWFGNiTi. *Scale bar*: 100 µm. ENRWFGNiTi, EGF, R-spondin1, Noggin, Wnt, FGF10, gastrin, nicotinamide, and TGFβ-inhibitor.

Supplementary Figure 3. Quantification of directed differentiation into gland and pit lineages. Cultures were grown in either ENRWFG_Ti to receive complete-type organoids (*left panel*), grown in ENRWFGNiTi to receive gland-type organoids (*middle panel*), or first kept in ENRWFGNiTi for 10 days and subsequently in ENR_FGNiTi for 4 days to receive pit-type organoids (*right panel*). Organoids were fixed, embedded in paraffin, and immunostained for the indicated markers. Positive cells and counterstained nuclei were counted blindly in 7 images per condition. Each image contained at least one organoid and, in total, at least 500 cells were counted per cell type. *Bars* represent averages of 7 images with standard deviation. SST-positive cells are very rare. Most randomly taken images do not contain SST-positive cells, but they can be found in each condition. ENRWFGNiTi, EGF, R-spondin1, Noggin, Wnt, FGF10, gastrin, nicotinamide, and TGFβ-inhibitor.

Supplementary Figure 4. *H pylori* infection of human gastric organoids. (*A*) Bacteria can be cultured from infected organoids. Two hours after microinjection of bacteria into organoids, single infected organoids were picked, lysed, and bacteria was plated out in serial dilutions. (*B*) Viability of bacteria in the inoculum and after 2 hours of infection in the organoids. Bacteria in the inoculum were quantified by plating out serial dilutions (*left panel*). Each organoid was injected with approximately 0.2 μL medium containing bacteria. After injection, bacteria were cultured back from the organoids as described in panel *A* and also quantified (*right panel*). *Bar* represents an average of 8 organoids with standard deviation. CFU, colony forming units. (*C*) IL8 messenger RNA (mRNA) induction depends on the MOI. Bacteria were injected at the indicated MOI, and mRNA levels of IL8 were assessed with quantitative PCR. (*D*) Induction of IL8 mRNA do not depend on either the bacterial pathogenicity island (*cag*PAI) or on viability of bacteria. Clinical isolate P12, its mutant P12Δ*cag*PAI, and heat-inactivated (h.i.) P12 were micro-injected, organoids were lysed after 2 hours, and induction of IL8 was assessed by quantitative PCR. (*E*) IL8 mRNA is induced by TNFα, IL1β, and flagellin, but not by LPS and CpG. Components were added to the medium and IL8 induction was assessed after 2 hours by quantitative PCR. (*D*) IL8 induction does not depend on *H pylori* flagellin or on bacterial motility. Clinical isolate G27, its aflagellated mutant G27Δ*fliG*, and its nonmotile mutant G27Δ*motB* were microinjected and the expression of IL8 mRNA was assessed by quantitative PCR. All mRNA was normalized to the glyceraldehyde-3-dehydrogenase (GAPDH) housekeeping gene. NI, noninfected organoid.

Supplementary Table 1. Genes Regulated by *H pylori* Infection

	Fold change	*P* value
CGB	14.56	.0048
CCL20	14.37	.0035
ICAM1	10.36	.0086
IL8	9.52	.0015
CYP3A5	3.94	.0461
TNFAIP3	3.78	.0208
CD83	3.44	.0139
BIRC3	3.23	.0132
IGKC	3.15	.0214
CXCL1	3.15	.0171
CHAC1	2.91	.0487
TNF	2.88	.0397
TNFRSF9	2.74	.0183
NAMPT	2.69	.0246
IL17C	2.61	.0483
NFKBIA	2.50	.0072
MIR146A	2.46	.0173
MIR4320	2.35	.0395
OR5M1	2.24	.0089
ZC3H12A	2.20	.0320
HIVEP2	2.16	.0437
IRAK2	2.06	.0437
C2orf16	−2.01	.0268
RNU6-57	−2.09	.0233
SNORA30	−2.33	.0126

NOTE. Organoid cultures from 3 patients were infected with *H pylori* at MOI of 50 for 2 hours. Genome-wide messenger RNA expression levels were analyzed with Affymetrix. The culture condition was ENRWFGNiTi.